Eur. Phys. J. B **58**, 237–242 (2007)
DOI: 10.1140/epjb/e2007-00231-3

THE EUROPEAN PHYSICAL JOURNAL B

An EPR study of Er^{3+} impurities in $RbTiOPO_4$ single crystals

D. Bravo[1,a], A. Martín[2], J.J. Carvajal[3], M. Aguiló[3], F. Díaz[3], and F.J. López[1]

[1] Departamento Física de Materiales, Universidad Autónoma de Madrid, Avda. Francisco Tomás y Valiente 7, Cantoblanco, 28049 Madrid, Spain
[2] Departamento Física e Instalaciones, ETS Arquitectura, Universidad Politécnica Madrid, Avda. Juan de Herrera 4, 28040 Madrid, Spain
[3] Física i Cristal·lografia de Materials (FiCMA), Universitat Rovira i Virgili (URV), Campus Sescelades, c/ Marcel·lí Domingo s/n, 43007 Tarragona, Spain

Received 29 March 2007 / Received in final form 16 July 2007
Published online 8 September 2007 –

Abstract. An electron paramagnetic resonance (EPR) study of Er^{3+} ions in single crystals of $RbTiOPO_4$ (RTP) is presented. The EPR spectra show the existence of six different Er^{3+} centres. The $\boldsymbol{g}$-matrix has been determined for these centres from the analysis of the angular dependences of the spectrum in three planes of the crystal. The study supports that erbium can enter the Rb^+ and Ti^{4+} low-symmetry sites of RTP. This conclusion differs from those for KTP:Er^{3+} and RTP codoped with Nb and Er. The different occupancies found for Er in these various crystals is suggested to be due to the differences in Er concentration.

PACS. 76.30.Kg Rare-earth ions and impurities – 42.70.Mp Nonlinear optical crystals

1 Introduction

Rubidium titanyl phosphate ($RbTiOPO_4$ or RTP) is an optoelectronic crystal, isostructural with the better-known Potassium titanyl phosphate ($KTiOPO_4$ or KTP). Both materials present high nonlinear optical coefficients, high optical damage threshold, and thermally stable phase-matching properties [1,2]. In recent years, RTP crystals have attracted a great attention since they can be grown with a concentration of rare earth (RE) impurities three orders of magnitude higher than KTP crystals [3]. This is especially suitable to develop self-doubled solid-state lasers based on RE elements as laser-active impurities. In particular, Er-doped RTP is particularly attractive for application in optical communication devices due to the photoluminescence emission of Er^{3+} around 1.5 μm, which coincides with the low-loss window of standard optical communication fibbers [4].

In order to optimize the performance of devices based on Er-doped RTP it is very important to know the nature of the active centres involved, i.e., the valence of the impurities, their local symmetry and location in the crystal lattice. The electron paramagnetic resonance (EPR) technique has proven to be very useful to obtain such basic information for many materials. In fact, EPR has been already used in the isomorphous KTP to study a considerable variety of centres related to transition-metal-ion elements [5–12] and the RE element erbium [13]. Whereas, RTP has been scarcely studied by EPR. To our knowledge, only V^{4+} impurities have been investigated in RTP [14], as well as Ti^{3+} defects [15] and radiation-induced trapped hole centres [15,16]. With respect to the location in the crystal lattice, all transition-metal-ion impurities have been found by EPR at both Ti sites existing in the KTP and RTP structure (see next section), except for Pt^+ impurities in KTP, which have been suggested to be substituting for K^+ [12]. Finally, from an EPR study of erbium in KTP [13], we have proposed that erbium occupies both K sites for the eight Er^{3+} centres analyzed.

As above mentioned, no EPR works of RE-doped RTP exist in the literature. The spectroscopic properties of this material doped with Er or Yb have been investigated by optical absorption and luminescence [3,17] in samples co-doped with Nb, which allows increasing the RE content. In these works it has been proposed that RE impurities coexist in various environments. Also, a neutron diffraction study of the structure of $RbTi_{0.927}Nb_{0.056}Er_{0.017}OPO_4$ crystals [18] concluded that Er enters the Ti sites only. This result diverges from the proposal mentioned above for Er^{3+} in KTP studied by EPR [13]. In this last work, we pointed out that such disagreement could be due to the large difference in Er content (two orders of magnitude) between both kind of crystals studied and the possible influence of Nb^{5+} ions. It must be noted that substitution for P has not been considered in any work, mainly due to the large size mismatch between RE^{3+}-elements and P^{5+} [19,20].

[a] e-mail: david.bravo@uam.es

In the present work we have employed the EPR technique to carry out a study of Er-doped RTP single crystals, analogous to that for Er^{3+} in KTP [13]. Up to six different centres have been identified and their $\boldsymbol{g}$-matrices have been determined. From this study we are proposing the location of the Er^{3+} ions at the Rb and Ti sites, in contrast to the proposal for KTP.

2 Experimental details and crystal structure

Single crystals of Er-doped RTP have been grown by the Top Seeded Solution Growth method. A solution with a molar composition Rb_2O-P_2O_5-TiO_2-Er_2O_3 = 45.00-30.00-23.75-1.25 has been employed. Crystals were grown by applying slow cooling of the solution for 1.5 K from the saturation temperature at a cooling rate of 0.1 K/h, and for additional 15.5 K at a cooling rate of 0.05 K/h. The crystals obtained showed the standard morphology of RTP crystals, with typical dimensions of $3 \times 6 \times 12$ mm^3 along a, b, and c crystallographic directions, respectively. Additional details about crystal growth and spectroscopic characterization of these crystals have been published elsewhere [21]. Erbium concentration has been measured by Electron Probe Microanalysis, giving a mean value of $(2.0 \pm 0.3) \times 10^{19}$ cm^{-3}. Prismatic samples, with dimensions $2 \times 2 \times 4$ mm^3, were oriented by using a D5000 Siemens X-ray diffractometer equipped with an open Eulerian cradle and cut with their faces perpendicular to the crystallographic axes a, b and c. The samples were mounted on a goniometer for measurements of the angular dependence of the EPR spectra.

EPR spectra have been recorded at 5 K using a Bruker ESP 300E X-band spectrometer with field modulation of 100 kHz. The temperature of the sample was controlled with an Oxford ESR 9 He-flux cryostat. Accurate values for the frequency and magnetic field were measured using a microwave-frequency counter (Hewlett-Packard 5342A) and a NMR gaussmeter (Bruker ER 035M), respectively.

The crystal structure of RTP is the same as that of KTP [22]. It is orthorhombic, with space group $Pna2_1$ and lattice parameters a = 12.974(2) Å, b = 6.494(3) Å and c = 10.564(6) Å [23]. There are two crystallographically distinct sites for each cation in the unit cell (labelled as Ti1, Ti2, Rb1, Rb2, P1 and P2) and ten independent oxygen sites (labelled as O1-O8, OT1 and OT2). All those sites have point symmetry C_1. To complete the structure within the unit cell, each ion has to be replicated in four positions by the symmetry operations of the space group (identity, two glide planes perpendicular to axes a and b, respectively, and one twofold screw axis parallel to axis c). Accordingly, the unit cell consists of eight formula $RbTiOPO_4$. Distances and polar coordinates of the oxygen ligands for cation sites Ti1, Ti2, Rb1 and Rb2, are given in Table 1.

It must be noted that rubidium Rb1 is eight-fold coordinated by oxygen, Rb2 is nine-fold coordinated and Ti1 and Ti2 are sixfold-coordinated. TiO_6 octahedra are linked by oxygens OT1 and OT2, whereas the remaining oxygen ligands belong to phosphate groups. It must be also remarked that the C_1 local symmetry of the TiO_6 octahedra can be approximated to tetragonal C_{4v} symmetry. This is because in each octahedron there is a shorter (≈1.72 Å) "titanyl" bond compared to the remaining Ti-O bonds (see Tab. 1). The shortest-bond direction would indicate the approximate four-fold axis.

Table 1. Distances d (Å) and polar angles θ and ϕ (deg) for Ti-O and Rb-O bonds in RTP, referred to the crystal (a, b, c) system. Errors are estimated to be one unit in the last digit.

$(Ti1)O_6$	d	θ	ϕ	$(Ti2)O_6$	d	θ	ϕ
O1	2.146	136.5	354.7	O3	2.064	98.2	348.0
O2	1.950	49.8	10.0	O4	2.011	86.1	173.0
O5	2.077	102.5	85.2	O7	1.967	48.1	270.6
O6	2.032	85.1	275.3	O8	1.988	141.7	87.7
OT1	1.974	140.6	191.7	OT1	1.737	49.0	72.9
OT2	1.714	47.8	167.0	OT2	2.094	134.5	257.0
$(Rb1)O_8$	d	θ	ϕ	$(Rb2)O_9$	d	θ	ϕ
O1	3.036	51.5	303.6	O1	2.748	106.2	125.8
O2	2.746	102.2	308.6	O2	3.105	48.7	131.6
O3	2.774	79.9	85.3	O3	3.117	2.2	144.9
O5	3.002	3.4	86.2	O4	3.053	124.7	266.9
O7	3.210	49.3	136.3	O5	2.867	83.1	180.4
O8	2.838	105.9	230.9	O7	2.999	100.8	50.6
OT1	3.163	52.6	236.5	O8	3.134	53.8	43.0
OT2	2.787	104.2	141.3	OT1	2.797	105.2	326.2
				OT2	3.111	51.4	336.7

3 Results

The EPR spectrum of Er-doped RTP samples, measured at 5 K, is composed of various groups of lines. Each group consists of a strong peak, near the centre of the group, and a number of satellite lines of much weaker intensity. The resonances appear in a wide magnetic field range from 400 G up to 8000 G. Typical peak-to-peak line-widths are 10 G for lines near 400 G and 100 G for lines near 3500 G. All lines remain observable up to ∼18 K, which is the usual behaviour for rare earth ions. For special orientations of the magnetic field $\boldsymbol{B}$ with respect to the crystallographic axes of RTP several groups collapse giving rise to simpler spectra. The EPR spectrum for $\boldsymbol{B}$ parallel to axis a is shown in Figure 1. A detailed inspection of the spectra for $\boldsymbol{B}$ parallel to the crystallographic axes a, b and c, reveals that they are composed of six intense groups. There are some other much weaker groups that cannot be followed along the angular dependences described below, and have not been analyzed. These have been marked with arrows in Figure 1.

The structure of each group (a strong peak and various satellite lines) is in agreement with the natural abundance ratio of the erbium isotopes. Thus, the strong peaks would be related to the 77.1% abundant even isotopes with zero nuclear spin, while the satellite components would correspond to the hyperfine (hf) structure arising from the

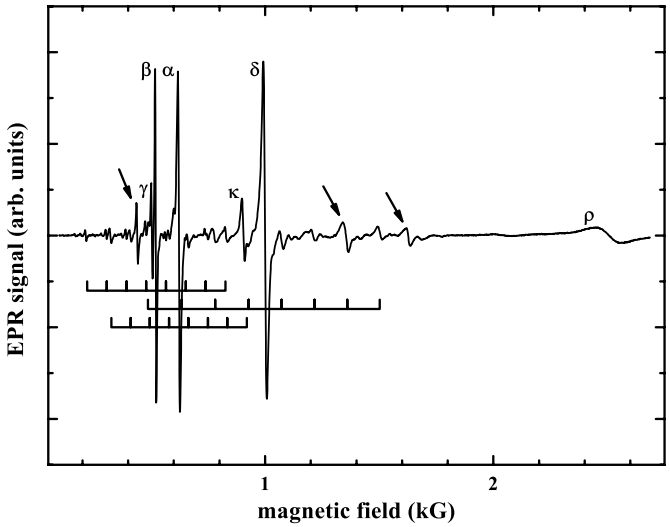

Fig. 1. EPR spectrum of an Er-doped RTP sample measured at 5 K with the magnetic field $\boldsymbol{B}$ oriented along axis a. Six even-isotope lines have been labelled α, β, γ, δ, κ and ρ, corresponding to the six Er^{3+} centres analyzed in Section 4. In the lower part, three calculated eight-line patterns, given in Table 2, have been drawn for the hf structure of centres α, β and δ, as described in Section 4. Arrows indicate lines from centres not studied here.

$I = 7/2$ nuclear spin of the ^{167}Er isotope, which is 22.9% abundant. According to this, the satellite lines show an eight-line pattern corresponding to the normal "allowed" transitions where the nuclear magnetic moment does not change, as marked in Figure 1 for the three clearest groups. Therefore, as confirmed in next paragraphs, we can attribute most of the observed spectrum to six trivalent erbium centres labelled α, β, γ, δ, κ and ρ. As usual for the Er^{3+} ion in crystal fields of symmetry lower than cubic, EPR signals are observed only for the lowest lying Kramers doublet of the $^4I_{15/2}$ free-ion ground level [13, 24]. So, the EPR spectra can be described in an effective $S' = 1/2$ notation. This means that each group of lines should be attributed to a particular orientation of an Er^{3+} related centre.

The angular dependence of the resonance line positions in the EPR spectra has been studied with the magnetic field $\boldsymbol{B}$ varying in the three crystallographic planes, i.e. planes ab, bc and ca (see Fig. 2). For simplicity only the intense even isotope lines have been plotted as open circles. When the magnetic field deviates in each plane from a, b or c axes, each line splits into two, as can be observed in Figure 2. Moreover, if the magnetic field is tilted out of the plane the lines split again into two giving 4 even-isotope lines for each centre. This behaviour agrees with the symmetry properties of the RTP lattice given above.

4 Analysis and discussion

To analyze the EPR spectra and their angular dependences the appropriate spin-Hamiltonian for an effective spin $S' = 1/2$ and nuclear spin $I = 7/2$ is [24]

$$\hat{H} = \mu_B \, \vec{B} \, \hat{g} \, \hat{\vec{S}}' \; + \; \hat{\vec{S}}' \, \hat{A} \, \hat{\vec{I}} \; - \; g_n \, \mu_n \, \vec{B} \, \hat{\vec{I}}, \qquad (1)$$

where the three terms represent the electronic Zeeman interaction, the hyperfine interaction and the nuclear Zeeman interaction, respectively. The last term has been neglected since it is small and gives corrections to the EPR lines positions below experimental error.

Table 2. Experimental and calculated resonance field values (Gauss) of eight-line patterns for the hf structure of centres α, β and δ with the magnetic field $\boldsymbol{B}$ oriented along axis a (see Fig. 1).

Centre		hf allowed transitions							
β	**Exper.**	214	304	391	478	564	–	740	829
	Calc.	220	306	393	479	566	653	739	826
α	**Exper.**	323	410	–	579	661	744	829	912
	Calc.	327	411	495	579	664	749	834	920
δ	**Exper.**	496	–	777	–	1072	1210	1355	1504
	Calc.	487	635	782	927	1072	1217	1360	1502

It must be noted that only the intense even-isotope lines can be followed along the whole range of study of the angular dependences, so that the hyperfine structure cannot be analyzed. Despite of this, we have employed the first two terms of equation (1) to calculate the three hf groups of eight-line patterns shown in Figure 1 and given in Table 2. This may confirm that they correspond to Er^{3+} ions. To this aim, we have used the $\boldsymbol{g}$-matrices for centres α, β and δ resulting from the analysis and fitting procedure given in next paragraph, taking $\boldsymbol{B}$ parallel to axis a. The corresponding $\boldsymbol{A}$-matrices have been constructed assuming they have the same principal axes as the $\boldsymbol{g}$-matrices. The principal $A-$values of each centre have been estimated from the following relationships: $A_X/g_X = A_Y/g_Y = A_Z/g_Z = A_J/g_J$, where $A_J = -125$ MHz is the magnetic hyperfine constant of the ^{167}Er isotope for the $^4I_{15/2}$ free-ion ground level of Er^{3+} and $g_J = 1.2$ is the Landé g-factor [24]. The matrix for the first two terms of equation (1) is then constructed with a computer program for $\boldsymbol{B}$ parallel to axis a and one value of B. The program also diagonalizes it and repeats the procedure for many values of B. By this method we can calculate energy levels and wavefunctions chosen within the spectrum range and obtain all possible hf transitions, as well as their intensity. The most intense transitions correspond to the normal "allowed" transitions which give rise to a simulated eight-line pattern for one centre. These have been drawn in Figure 1 for centres α, β and δ and are given in Table 2 together with the experimental values. As observed, the simulated patterns agree to a good extent with the experimental ones for the three centres, despite the assumptions made and the errors in the experimental positions due to their linewidth and line overlapping problems. This confirms that they correspond to Er^{3+} ions.

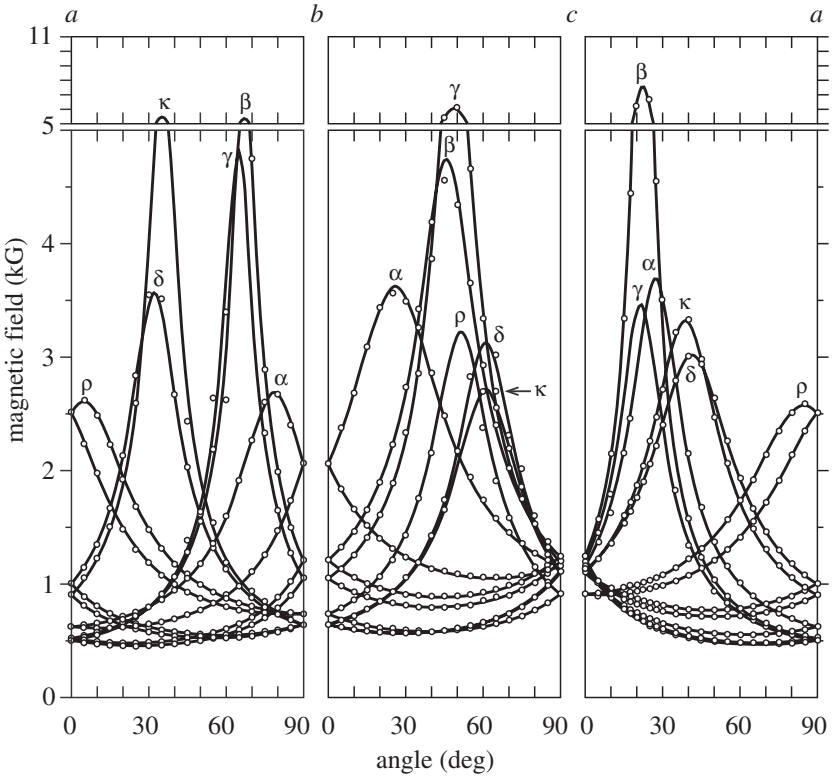

Fig. 2. Angular dependence of the EPR spectrum of centres α, β, γ, δ, κ and ρ in crystal planes *ab*, *bc* and *ca* of RTP. Experimental resonance-field positions of even-isotope lines are plotted with open circles. Calculated angular dependences are plotted with continuous lines.

On the other hand, to determine the $\boldsymbol{g}$-matrices for the six centres only the electronic Zeeman interaction is left in the Hamiltonian of equation (1). Another computer program has been used to construct and diagonalize the corresponding energy matrix for a number of magnetic field orientations taken for the data shown in the three angular dependences of Figure 2. The program also performs a least-squares fitting procedure to the experimental even-isotope line positions in such angular dependences. In the current study, an average of 90 independent line positions was used for each centre as input data, along with the corresponding microwave frequencies. The resulting best-fit matrices are shown in diagonal form in Table 3. Errors in the matrix elements shown in Table 3 are obtained from the used least-squares procedure by considering a 6 G uncertainty in the measured line position. Subsequently, the matrices are used to calculate the solid lines depicted in Figure 2. As observed, the agreement between experiment and theory is very good.

It must be pointed out that the diagonal elements of the $\boldsymbol{g}$-matrix have been assumed positive since their absolute and relative signs cannot be determined by usual EPR spectroscopy [24,25]. This aspect has been discussed in more detail in the previous work [13]. Each best-fit matrix for each centre represents four matrices, which are related to the four equivalent orientations of the corresponding centre in the RTP lattice (see Sect. 2). For the diagonal form of the matrices, this means that if the orientation of one principal axis for one centre is described by the direction cosines [l, m, n], the three other orientations of this axis are [-l, m, n], [l, $-m$, n] and [$-l$, $-m$, n]. For further discussion below, note that in terms of polar angles θ and ϕ the four orientations have the same θ value and different ϕ value.

The assignment of the observed EPR spectra to defects associated to Er^{3+} is also supported by the experimental mean g-value $(g_X + g_Y + g_Z)/3$. These mean values range from 5.43 to 6.25 for the six centres (Tab. 3), which are typical values for Er^{3+} in several hosts, with values ranging from 5.1 to 6.8 [24].

With regard to the location of Er^{3+} ions, there are four cation sites where erbium can enter, two Ti^{4+} sites and two Rb^{+} sites, as described in Sections 1 and 2. These sites have point symmetry C_1, which imposes a strong handicap to the EPR method in order to determine the location of impurities in any host with such low symmetry sites, since the principal axes of the magnetic interactions (Zeeman term and $\boldsymbol{g}$-matrices in the present case) do not hold a simple relationship with the arrangement of ligands. Fortunately, Ti-sites in KTP and RTP have a pseudo four-fold axis along the shortest titanyl bond (see Sect. 2). This has been used to locate most transition-metal impurities already studied by EPR in KTP [5–12] and RPT [14] at both Ti^{4+} sites, as they present nearly axial magnetic interactions along such bonds.

Table 3. Diagonal form of fitted $\boldsymbol{g}$-matrices for Er^{3+} centres α, β, γ, δ, κ and ρ observed in RTP at 5 K. Errors are shown in brackets for the last digit. Principal axes X, Y and Z are referred to the crystal (a,b,c) system. For a better comparison among directions for the different centres, all shown axes have $\theta < 90$ deg by changing the sign of direction cosines of those axes initially with $\theta > 90$ deg

Centre	Principal values	Mean g-value	Principal directions	
			θ	ϕ
α	$g_X = 1.17$ (1)	5.43 (1)	38.4 (2)	241.7 (2)
	$g_Y = 2.78$ (1)		65.0 (2)	115.8 (1)
	$g_Z = 12.35$ (1)		62.8 (1)	11.9 (1)
β	$g_X = 0.613$ (6)	5.690 (5)	41.3 (2)	138.6 (2)
	$g_Y = 1.471$ (3)		56.3 (2)	278.1 (1)
	$g_Z = 14.985$ (6)		69.1 (1)	22.8 (1)
γ	$g_X = 0.909$ (1)	6.246 (2)	58.1 (1)	282.3 (1)
	$g_Y = 2.107$ (2)		39.0 (1)	142.17 (1)
	$g_Z = 15.723$ (2)		70.0 (1)	25.4 (1)
δ	$g_X = 1.851$ (1)	5.878 (1)	74.4 (1)	320.5 (1)
	$g_Y = 2.268$ (1)		30.0 (1)	201.6 (1)
	$g_Z = 13.514$ (1)		65.1 (1)	58.0 (1)
κ	$g_X = 0.3$ (1)	5.5 (1)	57 (2)	308 (2)
	$g_Y = 2.04$ (9)		43 (2)	175 (2)
	$g_Z = 14.1$ (1)		65.1 (6)	55.1 (3)
ρ	$g_X = 2.04$ (3)	5.43 (2)	41.9 (3)	293 (2)
	$g_Y = 2.638$ (6)		76 (1)	187 (1)
	$g_Z = 11.60$ (3)		51.6 (1)	85.5 (1)

On the other hand, RE ions Yb^{3+} and Er^{3+} in RTP [3,17] have been assumed to be located at Ti^{4+} sites (see Sect. 1). In this work, we are using the resulting matrices in Table 3 to propose the location of Er^{3+} in RTP. First, it must be noted that the principal values for most centres shown in Table 3 indicate a strong axial character, the Z-axis being assigned to the largest principal g-value. Therefore, the most direct method one can try to locate Er^{3+} is to extrapolate the former idea for transition-metal impurities to this rare-earth ion. So, one could expect principal axis Z being close to the direction of some of the cation-oxygen bonds. In fact, in the case of Er^{3+} in KTP [13] such kind of comparisons enabled the most reliable assignment of the eight studied Er centres to the K sites despite their low C_1 site-symmetry, noting that substitution for Ti was not fully excluded. For the present case of Er in RTP, one can also compare each Z-axis for the six centres in Table 3 to Ti-O and Rb-O bond directions shown in Table 1.

For the sake of an easier comparison, we can work with all directions in the first octant of the Euclidean three-dimensional coordinate system. So, directions with $\theta > 90$ deg are changed in first place by the inversion symmetry operation since the EPR spectrum is invariant under this operation [24]. In addition, directions with $\phi > 90$ deg are changed using the appropriate symmetry operation of the space group $Pna2_1$ (see Sect. 2). Thus, one can take the shortest "titanyl" bond directions in Table 1 approximately as $\theta = 48$ deg and $\phi = 13$ deg for Ti1-OT2, and $\theta = 49$ deg and $\phi = 73$ deg for Ti2-OT1. On the other hand, Rb-O bond directions for both Rb1 and Rb2 sites can be grouped into two families whose polar angles θ are near 52 and 76 deg (180–104 deg), having ϕ values around 50 deg or 30 deg for most directions. As can be seen in Table 3, centres β and γ have very similar Z-axes with θ near 70 deg, which compares better to 76 deg of Rb sites than to 48 or 49 deg of Ti sites. So, we propose centres β and γ as Er^{3+} substituting for Rb^{+}. Also, centres δ and κ have very close Z-axes with θ near 65 deg and ϕ near 56 deg, far from $\phi = 13$ deg or 73 deg for the "titanyl" bonds. Therefore we also propose these two centres to be substituting for Rb^{+}. However, centre α would be a good candidate for an erbium centre at the Ti1 site, since its Z-axis has θ near 63 deg and ϕ near 12 deg. Finally, the assignment for centre ρ is less clear, since its Z-axis has θ near 52 deg and ϕ near 86 deg, which could be ascribed to the Ti2-OT1 bond or also to the Rb2-O4 bond, with θ near 55 deg and ϕ near 87 deg (Tab. 1).

Analogous comparisons for Er in KTP [13] were easier than the above for RTP and all centres could be assigned to the K^{+} sites. In contrast, the results in this work would indicate that Er^{3+} ions can enter both kind of sites in RTP, in accordance with the optical studies [3,17] and neutron diffraction study [18] of Nb-codoped RTP. We suggest that the origin for the different occupancies proposed in all these works is related to the different Er concentration in the crystals used in each work. Low Er concentrations as in KTP [13] would produce crystals with Er located mainly at the K sites. RTP crystals here studied contain 10 times more Er than in KTP [13] and Er seems to occupy Rb and Ti sites. Finally, RTP crystals co-doped with Nb [18] contain 10 times more Er than our single-doped RTP crystals, and in such case most Er would be located at the Ti sites.

Finally, it should be noted that charge compensation must exist since we are considering substitution of Rb^{+} or Ti^{4+} by a trivalent ion. In fact, we are proposing at least four different Er^{3+} centres at only two Rb^{+} sites in the lattice. A reliable explanation for this is to assume some site perturbation related to the compensation of the charge misfit between Er^{3+} and Rb^{+}, which can be reached through Rb^{+} vacancies close to Er^{3+} ions.

This work has been supported by DGESIC and CICyT under projects BFM2001-0221, MAT2002- 04603, CIT-020400-2005-14 and MAT2005-06354-C03-02.

References

1. M.E. Hagerman, K.R. Poeppelmeier, Chem. Mater. **7**, 602 (1995)
2. M.N. Satyanarayan, A. Deepthy, H.L. Bhat, Crit. Rev. Solid State Mater. Sci. **24**, 103 (1999)
3. J.J. Carvajal, R. Solé, Jna. Gavaldà, J. Massons, M. Aguiló, F. Díaz, Optical Materials **24**, 425 (2003)

4. P.C. Becker, N.A. Olsson, J.R. Simpson, *Erbium-Doped Fiber Amplifiers: Fundamentals and Technology*, (Academic Press, San Diego, 1999)
5. J.M. Gaite, J.F. Stenger, Y. Dusausoy, G. Marnier, H. Rager, J. Phys.: Condens. Matt. **3**, 7877 (1991)
6. S.W. Ahn, S.H. Choh, J. Phys.: Condens. Matt. **11**, 3193 (1999)
7. A.B. Vassilikou-Dova, S. Jansen, F. Wallrafen, G. Lehmann, Z. Naturforsch. A **44**, 711 (1989)
8. S. Han, J. Wang, Y. Xu, Y. Liu, J. Wey, J. Phys.: Condens. Matt. **4**, 6009 (1992)
9. I.N. Geifman, A.N. Usov, P.G. Nagornyi, Phys. Stat. Sol. B **172**, K73 (1992)
10. D. Bravo, M.J. Martín, Jna. Gavaldà, F. Díaz, C. Zaldo, F.J. López, Phys. Rev. B **50**, 16224 (1994)
11. D. Bravo, X. Ruiz, F. Díaz, F.J. López, Phys. Rev. B **52**, 3159 (1995)
12. N.Y. Garces, K.T. Stevens, L.E. Halliburton, J. Appl. Phys. **87**, 8682 (2000)
13. D. Bravo, A. Martín, J.J. Carvajal, M. Aguiló, F. Díaz, F.J. López, J. Phys.: Condens. Matt. **18**, 6655 (2006)
14. I.N. Geifman, I.S. Golovina, P.G. Nagornyi, Phys. Solid State **40**, 491 (1998)
15. M.A. Laruhin, V.N. Efimov, V.A. Nazarova, G.R. Bulka, Appl. Magn. Reson. **15**, 247 (1998)
16. Y. Jiang, L.E. Halliburton, M. Roth, M. Tseitlin, N. Angert, Phys. Stat. Sol. B **242**, 2489 (2005)
17. J.J. Carvajal, R. Solé, Jna. Gavaldà, J. Massons, M. Rico, C. Zaldo, M. Aguiló, F. Díaz, J. Alloys, Compounds **323–324**, 231 (2001)
18. J.J. Carvajal, J.L. García-Muñoz, R. Solé, Jna. Gavaldà, J. Massons, X. Solans, F. Díaz, M. Aguiló, Chem. Mater. **15**, 2338 (2003)
19. C. Zaldo, M. Aguiló, F. Díaz, H. Loro, J. Phys.: Condens. Matt. **8**, 10693 (1996)
20. M. Rico, C. Zaldo, J. Massons, F. Díaz, J. Phys.: Condens. Matt. **10**, 10101 (1998)
21. C. Zaldo, M. Rico, J.J. Carvajal, F. Díaz, Opt. Mater. **13**, 175 (1999)
22. P.A. Thomas, A.M. Glazer, B.E. Watts, Acta Cryst. B **46**, 333 (1990)
23. P.A. Thomas, S.C. Mayo, B.E. Watts, Acta Cryst. B **48**, 401 (1992)
24. A. Abragam, B. Bleaney, *Electron Paramagnetic Resonance of Transition Ions* (Clarendon/Oxford University Press, New York, 1970)
25. J.R. Pilbrow, M.R. Lowrey, Rep. Prog. Phys. **43**, 433 (1980)